Inorganica Chimica Acta 510 (2020) 119680

Contents lists available at ScienceDirect

Inorganica Chimica Acta

journal homepage: www.elsevier.com/locate/ica

Research paper

Mercury (II) sensing via cyclization of a dithioamide into a benzimidazole derivative: A structural and spectroscopic study

Adenike O. Fasiku, Matthew T. Fortunato, Indranil Chakraborty*, Konstantinos Kavallieratos*

Department of Chemistry and Biochemistry and Biomolecular Sciences Institute, Florida International University, Miami, FL 33199, United States

ARTICLE INFO

Dedicated to the memory of Professor Tara P. Dasgupta.

Keywords:
Benzimidazole synthesis
Mercury sensor
Thioamide
Mercury-catalyzed cyclization

ABSTRACT

An *o*-phenylenediamine-derived dithioamide **L** was found to sense Hg(II) in the UV–visible via Hg(II)-mediated cyclization leading to a new benzimidazole derivative (**L′**). Both **L** and **L′** have been characterized by single-crystal X-ray crystallography. The structure of **L** reveals relatively strong intramolecular H-bonding interactions of N—H...S type. The extended structure is consolidated by several classical hydrogen bonding interactions. For **L′**, analysis of the packing pattern reveals few non-classical H-bonding contacts. Spectroscopic studies by FT-IR, UV–Visible, ^{1}H-and ^{13}C NMR support the single-crystal X-ray crystallography results and confirm the formation of the new benzimidazole derivative. UV–Vis titrations suggest and NMR confirms that the cyclization reaction occurs via an initial formation of a Hg(II) complex, which is too transient to be fully characterized. As this reaction is Hg(II)-mediated, dithioamide **L** acts as a selective Hg(II) sensor as shown by UV–Visible titrations and a selectivity study against Pb(II), Cd(II), Ca(II), Zn(II), Ag(I), and Cr(III): For Hg(II), but not for other metals, a distinct color change from yellow to pink is observed with corresponding UV–Vis spectroscopic changes and an isosbestic point at 270 nm.

1. Introduction

Mercury is a pollutant arising from both natural and anthropogenic sources mainly through medicinal and industrial applications. The very toxic organic forms of mercury have some lipophilicity and can pass through the blood brain barrier, thus causing short-term and long-term detrimental effects to human brain, and also to lungs and kidneys [1]. Hg(II) is an environmentally mobile form of Hg and can be transformed into more toxic organic forms. Hence, developing methods to sense both Hg(II) and organic mercury in the environment is of great importance. Over the years, various detection methods for mercury in the environment have been widely studied including atomic absorption, fluorescence sensing, electrochemical sensing and colorimetric methods [2]. Low-cost colorimetric and fluorescence sensors offer the potential for high sensitivity and selectivity for detection of Hg(II) in environment [3–8].

Our group has been engaged in developing sulfonamide and carboxamide-based extractants for sequestration and sensing of toxic metals ions, such as Pb(II) [9–11] and f-elements [12]. As we were studying the Hg(II) complexation properties of dithioamide (**L**) with $HgCl_2$/$Hg(CH_3COO)_2$ we noticed that no Hg(II) complex with **L** could be isolated from the reaction, but instead a new benzimidazole derivative (**L′**) was formed via Hg(II)-mediated cyclization. Owing to their wide range of applications in pharmaceutical industries, benzimidazole derivatives are considered as an important class of heterocyclic compounds. One of the most common examples of existence of benzimidazole derivative in nature is *N*-ribosyl-dimethylbenzimidazole, which binds the Cobalt center axially in Vitamin B_{12} [13]. Based on their biological evaluations, several benzimidazole derivatives have also find their place as anti-microbial, anti-hypertensive, anti-viral and anti-ulcer agents within clinical settings [14–19]. In recent times the prevailing antimicrobial resistance is an alarming issue worldwide, especially as a sizeable number of multi drug resistant (MDR) pathogens have been found to render the action of some crucial antimicrobial agents (like *β*-lactam-based antibiotics, vancomycin, quinolones *etc*.) ineffective. This situation has triggered various research groups to develop smart ways of designing antibacterial agents to alleviate the resistance mechanisms inherent to these MDR pathogens. Due to structural similarity with purines, there is a considerable research interest to develop antimicrobial agents based on benzimidazole ligand frameworks. Although the direct synthetic methodology for preparation of benzimidazoles which involves *ortho*-di- aryl amine and an aldehyde are well known, this procedure often leads to several undesirable side products. Various metal-based catalysts, namely Cu, Co, Ru, Pd, Zn and Rh are known to afford much cleaner and sustainable results [20–24]. Mercury has also been reported as a catalyst that mediates these cyclization reactions

* Corresponding authors.
E-mail address: kavallie@fiu.edu (K. Kavallieratos).

https://doi.org/10.1016/j.ica.2020.119680
Received 17 December 2019; Received in revised form 7 April 2020; Accepted 15 April 2020
Available online 18 April 2020
0020-1693/

[6,25,26]. For instance, Su et al. developed a microwave- assisted technique for a $HgCl_2$-mediated synthesis of benzimidazole by intermolecular cyclization using triethylamine [27]. Wang et al. synthesized polysubstituted benzimidazoles from *ortho*-di-arylcarboxamides through electrophilic activation of amides with trifluoromethanesulfonic anhydride and 2-chloropyridine [28].

Herein, we are exploiting the capability of Hg(II) to catalyze the cyclization reaction of *o*-phenylenediamine-derived diamides to benzimidazoles to report a unique sensing method for Hg(II), which is reasonably selective against several competing metals. Furthermore, we have shown the utility of this Hg(II)-mediated reaction for a facile synthesis of a new fully characterized benzimidazole thioamide derivative, which is not straightforward by other conventional synthetic pathways.

2. Experimental

2.1. Materials and methods

All chemicals and materials were purchased from Fisher Scientific or Sigma-Aldrich. All chemicals were standard reagent grade and were used without further purification except for toluene, which was distilled from CaH_2 before use. NMR spectra were recorded on either a 400-MHz Bruker Avance or a 600-MHz Bruker Avance NMR spectrometer. The UV–Visible spectra were recorded on a CARY 100 Bio UV–Visible spectrophotometer. X-ray diffraction studies were carried out on a Bruker D8 Quest with PHOTON 100 detector. The diamide precursor (*N,N′*-(1,2-phenylene)dibenzamide) of **L** was synthesized by a modification of a previously-reported procedure [29] and was found spectroscopically identical to the reported compound [30]. The dithioamide ligand **L** has been previously reported [31], yet we have now synthesized it by a different method [32] and report its NMR characterization and X-ray structure.

2.2. Synthesis of N,N′-(1,2-phenylene)dibenzothioamide (L)

N,N′-(1,2-phenylene)dibenzamide (0.506 g (1.60 mmol) was dissolved in distilled dry toluene (100 mL). To this solution, 1.424 g (3.52 mmol, 2.2 eq.) of 2,4-Bis(4-methoxyphenyl)-1,3,2,4-dithia-diphosphetane-2,4-disulfide (Lawesson's Reagent) was added. The reaction mixture was then heated to reflux under nitrogen with constant stirring. After 30 min, the solution turned yellow. After 12 h, the volatiles were evaporated to dryness. A small volume of dichloromethane was used to dissolve the residue, which was subjected to *silica gel* column chromatography with hexane/ethyl acetate (7:3) as the eluent. The yellow-band eluted fraction was dried *in vacuo* and dissolved in a small volume of dichloromethane. Dropwise addition of hexanes and cooling at 4 °C gave a crystalline yellow precipitate, which was filtered, washed with hexanes, and dried under vacuum. Yield: 0.244 g (0.70 mmol, 43.8%); FT-IR (cm^{-1}): 3263, 1508, 1444, 1361, 1216, 987, 921; ^1H NMR (600 MHz, $CDCl_3$) δ 9.38 (s, 2H), 7.86 (d, J = 7.7 Hz, 4H), 7.64 – 7.60 (m, 2H), 7.56 – 7.51 (m, 2H), 7.48 (t, J = 7.4 Hz, 2H), 7.39 (t, J = 7.7 Hz, 4H); ^{13}C NMR (101 MHz, $CDCl_3$) δ 200.04 (s), 141.05 (s), 134.85 (s), 131.87 (s), 129.18 (s), 128.68 (s), 127.95 (s), 127.08 (s).

2.3. Synthesis of Phenyl(2-phenyl-1H-benzimidazol-1-yl)methanethione (L′)

N,N′-(1,2-phenylene)dibenzothioamide (**L**) (0.041 g, 0.12 mmol) was dissolved in methanol (20 mL) in a round-bottom flask. 42 μL (0.264 mmol) of N.N′-diisopropylethylamine (DIPEA) was added and the solution was left to stir for 5 min. A solution of $HgCl_2$ (0.032 g, 0.12 mmol) or $Hg(OAc)_2$ (0.038 g, 0.12 mmol) in methanol (5 mL) was added dropwise to the stirring solution of **L**. A pale yellow precipitate immediately formed. The reaction mixture was then heated to reflux. After 5 h, the reaction contained a pink solution with a black precipitate, which was filtered off by gravity filtration. The volatiles were evaporated under reduced pressure, and the pink residue was dissolved in methylene chloride and subjected to a silica gel column chromatography using methylene chloride as the mobile phase. The fraction containing the pink band was collected, dried under reduced pressure, and the resulting purple powder was recrystallized in CH_2Cl_2/hexanes, washed with hexanes, and dried under vacuum. Yield (based on $HgCl_2$): 0.025 g, (0.08 mmol, 66.6%); FT-IR (cm^{-1}): 1587, 1446, 1313, 1309, 1267, 1164, 1033; ^1H NMR (600 MHz, $CDCl_3$) δ 7.95 (d, J = 7.8 Hz, 1H), 7.68 (dd, J = 14.6, 7.3 Hz, 4H), 7.53 (d, J = 7.4 Hz, 1H), 7.42 (t, J = 7.7 Hz, 1H), 7.39 (d, J = 8.2 Hz, 1H), 7.34 – 7.27 (m, 6H); ^{13}C NMR (101 MHz, MeOD) δ 209.63 (s), 145.70 (s), 143.82 (s), 137.90 (s), 135.47 (s), 131.34 (s), 130.88 (s), 130.61 (s), 130.15 (s), 129.76 (s), 126.12 (s), 126.00 (s), 120.59 (s), 118.17 (s), 113.79 (s); *Anal.* Calc. for $C_{20}H_{14}N_2S{\cdot}1/6CH_2Cl_2$ (%): C 73.72, H 4.40, N 8.53. Found (%): C 73.83, H 4.43, N 8.53.

2.4. X-ray crystallography

The isolated **L** and **L′** were dissolved in methylene chloride and the solutions were layered carefully with hexanes. Yellow crystals of the dithioamide were formed after several days. Light purple crystals of the benzimidazole derivative were formed within a week. X-ray structure determination experimental details are summarized in Table 1. The non-H atoms are located through intrinsic phasing using *SHELXT* [33] integrated in the *Olex2* graphical user interface [34]. H-atoms are included in calculated positions riding on the C atoms to which they bonded, with C—H = 0.93 Å and *U*iso(H) = 1.2Ueq(C). The N—H hydrogen atoms are located within the difference map.

3. Results and discussion

3.1. Synthesis

The dithioamide **L** [31] was synthesized in two steps (Scheme 1) from commercially available *o*-phenylenediamine and benzoyl chloride in DMF [29] to give initially the diamide, which was subsequently reacted [32] with Lawesson's Reagent in dry toluene to give a yellow product, which was characterized by FT-IR, $^1H/^{13}C$ NMR, and X-ray crystallography. Even though **L** is known [31], the report is not easily accessible, and its X-ray structure is also reported here for the first time.

The benzimidazole thioamide derivative **L′** was synthesized by a Hg (II)-mediated cyclization reaction after reflux in CH_3OH using 1.2 eq. of $HgCl_2$ or $Hg(OAc)_2$. In a reaction similar to ours, Wang et al. have successfully synthesized different polysubstituted benzimidazoles from *ortho*-di-arylcarboxamides using trifluoromethanesulfonic anhydride and 2-chloropyridine as the reaction mediator [28]. Su et al. have also used a microwave-assisted Hg(II)-mediated cyclization to synthesize benzimidazoles using $HgCl_2$ and triethylamine [27]. Our reported cyclization reaction has now resulted to a new thioamide-benzimidazole derivative, and we also provide evidence -for the first time for this type of reactions- on the formation of a transient Hg(II)-**L** dithioamide complex. The reaction was carried out by dropwise addition of HgX_2 ($X = Cl^-$ or CH_3COO^-) in methanol to a stirring solution of ligand and DIPEA in methanol. The transient Hg(II) complex was formed immediately as a yellow powder and filtered, while the pink filtrate was dried *in vacuo* and recrystallized to obtain the cyclized product. The stability of the isolated transient Hg(II) complex both in solution and in solid state is poor, yet we were able to record the UV–Vis, FT-IR (Figs. S1 and S2), and ^1H NMR spectra (Fig. 7) immediately after synthesis, which already show the transient complex being transformed gradually to the cyclized benzimidazole product. As our group focuses on the complexation and sensing of mercury by sulfonamides and thioamides, this mercury-mediated cyclization reaction was further exploited for Hg (II)-selective sensing. For synthesis in a larger scale, we found out that

Table 1
Experimental details for X-ray structure determination.

	(**L**)	(**L′**)
Crystal data		
Chemical formula	$C_{20}H_{16}N_2S_2$	$C_{20}H_{14}N_2S$
M_r	348.47	314.39
Crystal system, space group	Triclinic, $P\bar{1}$	Triclinic, $P\bar{1}$
Temperature (K)	273	293
a, b, c (Å)	8.7208 (4), 10.0905 (5), 11.4131 (5)	8.9989 (7), 9.8812 (8), 9.9587 (8)
α, β, γ (°)	66.506 (1), 72.172 (1), 89.016 (1)	111.313 (2), 97.350 (2), 98.663 (2)
V (Å^3)	870.49 (7)	799.35 (11)
Z	2	2
Radiation type	Mo $K\alpha$	Mo $K\alpha$
μ (mm^{-1})	0.31	0.20
Crystal size (mm)	0.30 × 0.25 × 0.20	0.15 × 0.10 × 0.08
Data collection		
Diffractometer	Bruker D8 Quest with PHOTON 100 detector	Bruker D8 Quest with PHOTON 100 detector
Absorption correction	Multi-scan *SADABS2016/2* (Bruker, 2016/2) was used for absorption correction. w*R*2(int) was 0.0430 before and 0.0379 after correction. The Ratio of minimum to maximum transmission is 0.9450. The λ/2 correction factor is Not present.	Multi-scan *SADABS2016/2* (Bruker, 2016/2) was used for absorption correction. w*R*2(int) was 0.0598 before and 0.0480 after correction. The Ratio of minimum to maximum transmission is 0.8939. The λ/2 correction factor is not present.
T_{min}, T_{max}	0.705, 0.746	0.650, 0.745
No. of measured, independent and observed [$I > 2\sigma(I)$] reflections	17250, 4321, 3533	10067, 2726, 2003
R_{int}	0.020	0.031
(sin θ/λ)$_{max}$ (Å^{-1})	0.668	0.589
Refinement		
$R[F^2 > 2\sigma(F^2)]$, w$R(F^2)$, S	0.037, 0.102, 1.04	0.048, 0.135, 1.05
No. of reflections	4321	2726
No. of parameters	225	208
H-atom treatment	H-atoms treated by a mixture of independent and constrained refinement	H-atom parameters constrained
$\Delta\rho_{max}$, $\Delta\rho_{min}$ (e Å^{-3})	0.26, −0.37	0.32, −0.48

refluxing the reaction mixture for 5 h gives higher yields (up to 66.6%) for the formation of the benzimidazole derivative (**L′**) (Scheme 1). For growing suitable crystals for X-ray diffraction: Methylene chloride solutions of reaction mixtures of $HgCl_2$ and **L** were layered with hexanes. The solution color turned initially yellow, and eventually pink, with a black precipitate settled at the bottom of the tubes. This is presumably due to demetallation of the transient Hg(II)-**L** species, with the black precipitate being HgS (Scheme 2).

3.2. FT-IR studies

The infrared spectrum of the new benzimidazole derivative (**L′**) is characterized by the presence of three distinct bands at 1585, 1309, and 1162 cm^{-1} (Fig. 1). These bands are attributed to the stretching vibrations of the C═N, C−N and C═S respectively. Strong and medium intensity bands at 1600–1400 cm^{-1} correspond to the C═N and C═C stretching vibrations. Disappearance of the band corresponding to N−H

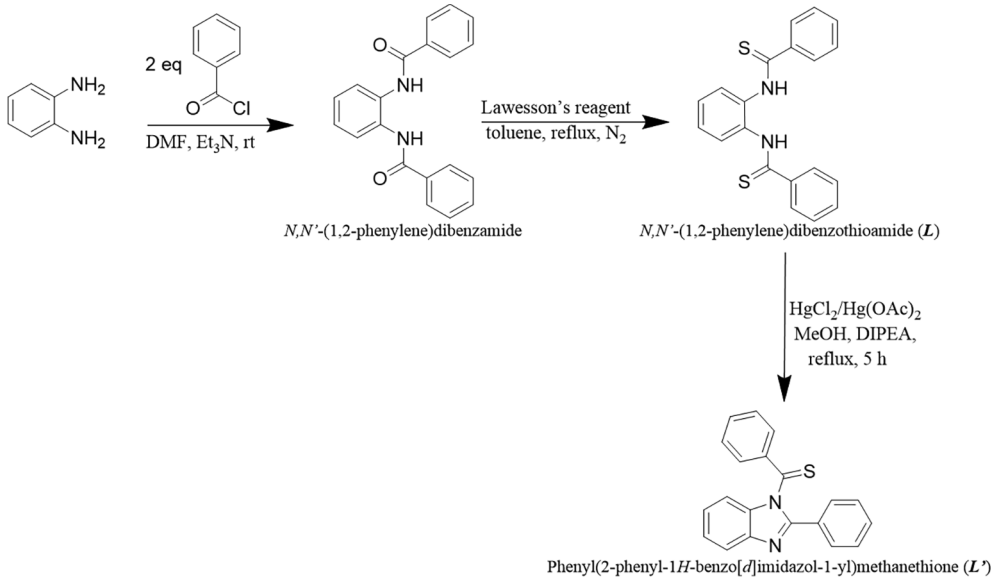

Scheme 1. Synthesis of *N,N′*-(1,2-phenylene)dibenzothioamide (**L**) and Phenyl(2-phenyl-1*H*-benzo[*d*]imidazole-1-yl)methanethione (**L′**).

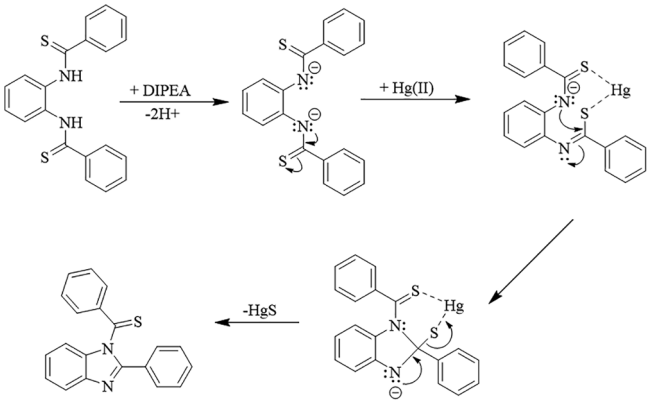

Scheme 2. Proposed mechanism of Hg(II)-catalyzed cyclization reaction transforming **L** into **L′**.

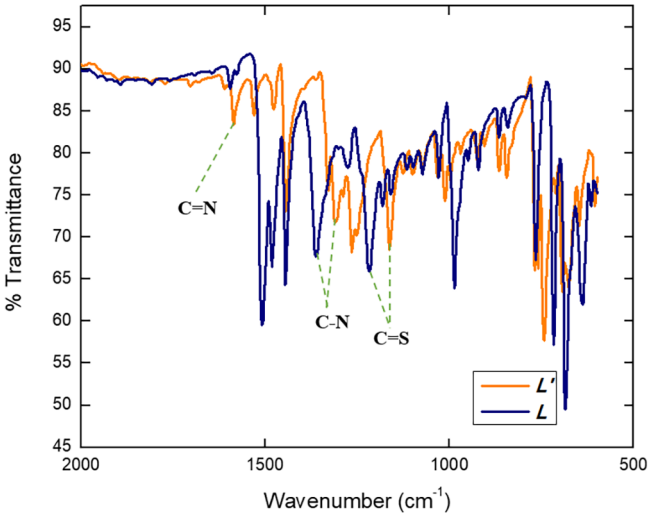

Fig. 1. FT-IR spectra of the dithioamide ligand (**L**) and the cyclized benzimidazole (**L′**).

stretching vibrations in the 3300–3000 cm^{-1} region of the ligand (**L**) spectra and the appearance of a new ν(C═N) band of medium intensity at 1585 cm^{-1} for **L′** indicates formation of the benzimidazole ring. In addition, shifts to lower frequency are observed for the ν(C═S) from 1216 cm^{-1}, in **L** to 1162 cm^{-1} in **L′**. A shift for the ν(C—N) band is also observed from 1365 cm^{-1}, in **L** to 1309 cm^{-1} in **L′**, which is also consistent with the formation of the benzimidazole.

3.3. UV–Visible sensing studies - titrations

The formation of the new benzimidazole derivative **L′** was also confirmed by UV–Vis spectroscopy. The absorption spectra of **L** and isolated **L′** were recorded in 0.1 mM MeOH solutions using a quartz cuvette of 1 cm path length (Fig. 2). Response to Hg(II) addition was monitored by gradual addition of various amounts of Hg(II) (0.005–1.600 mL of 0.5 mM $HgCl_2$) to solutions of **L** (0.02 mM) and DIPEA (0.044 mM) in MeOH (at constant concentration of **L** and DIPEA). A 10 min interval was used before each reading to ensure the reaction is under thermodynamic control. The UV–Vis spectra of dithioamide **L** in MeOH solution shows an absorption band at 248 nm. Addition of Hg(II) resulted in a red shift and a gradual disappearance of this absorption band (Fig. 3) with two new bands appearing at 286 nm and 328 nm, an observation consistent with formation of the

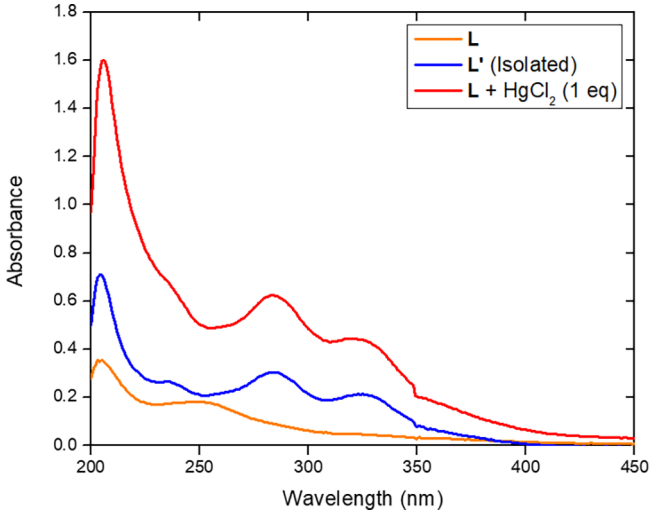

Fig. 2. UV–Vis spectra of i) **L** (0.1 mM) in MeOH, ii) isolated **L′** (0.1 mM) in MeOH and iii) reaction mixture after addition of $HgCl_2$ (1 eq., 0.1 mM) to **L** in MeOH, after standing for 24 h.

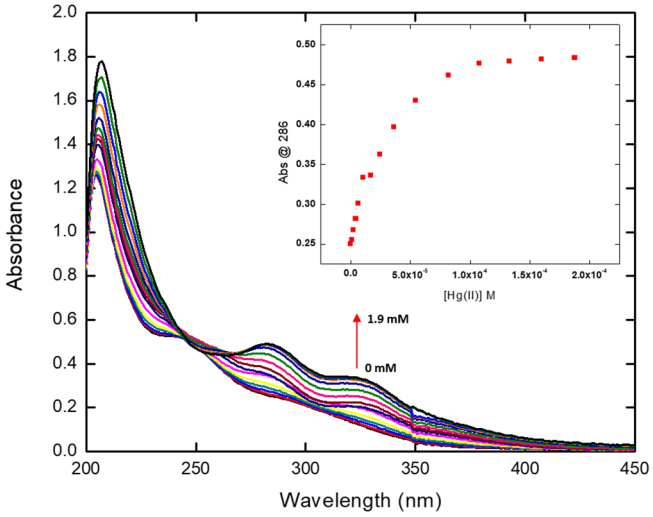

Fig. 3. UV–Vis titration of **L** (0.02 mM) and DIPEA (2.2 eq.) in CH_3OH after gradual addition of $HgCl_2$ (0.5 mM) at constant **L** and DIPEA concentration.

benzimidazole. Very similar spectra were obtained after the addition of $Hg(OAc)_2$ (Fig. S3 in Supporting Information section). The ratio changes observed in the titration plot (Fig. 3) produced a linear function for a Hg(II) concentration up to 10.63 μM. The detection limit was calculated to be 0.69 μM (see Supporting Information), with a 1.08 μM to 10.63 μM dynamic range. It is notable that the spectra of i) isolated benzimidazole product ii) the reaction mixture after 24 h, and iii) the titration spectra after Hg(II) addition, are virtually identical. This observation is consistent with the hypothesis that the UV–Vis sensing of Hg(II) is a direct result of the Hg(II)-mediated cyclization reaction.

Selectivity for Hg(II) sensing by **L** compares favorably vs. various other metals, including Cd(II), Pb(II), Zn(II), Ca(II), Ag(I), and Cr(III). 1 equivalent of these metals (added as chloride salts) was added to solutions of **L** (0.1 mM) and 2.2 eq of DIPEA and the solutions were left to stand for 24 h. The UV–Vis spectra were collected and are shown in Fig. 4 (for Cd(II), Pb(II), Zn(II), and Hg(II)), and in Fig. 5 (for Ca(II), Ag (I), Cr(III) and Hg(II)). Only for mercury addition the new benzimidazole bands at 286 nm and 328 nm appear prominently. Pb(II) and Cd

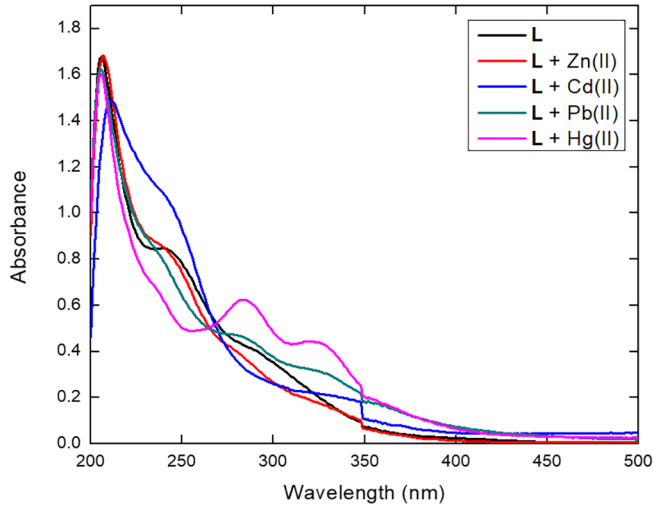

Fig. 4. UV–Vis spectra of **L** (0.1 mM) before and after addition of chloride salts of Zn(II), Pb(II), Cd(II), or Hg(II) (1 eq.) in MeOH after standing for 24 h.

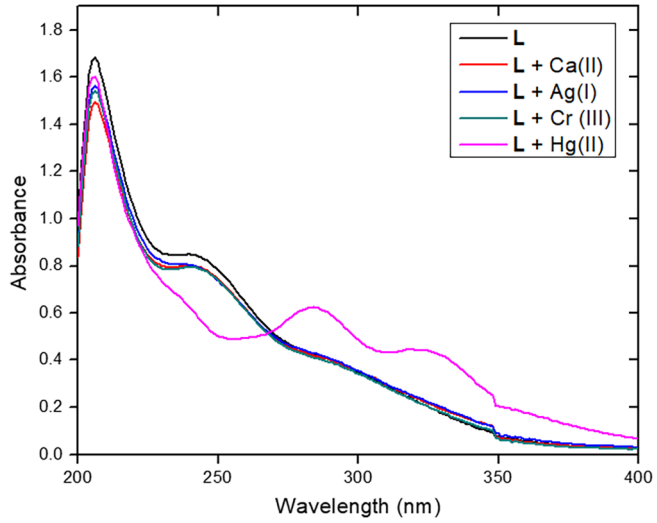

Fig. 5. UV–Vis spectra of **L** (0.1 mM) before and after addition of chloride salts of Ca(II), Ag(I), Cr(III), and Hg(II) (1 eq.) in MeOH, after standing for 24 h.

(II), show some increases in absorption (Fig. 4), which are more consistent with complex formation, rather than benzimidazole formation, while Zn(II), Ca(II), Ag(I) and Cr(III) show no interference (Figs. 4 and 5).

3.4. NMR spectroscopy

The ^{1}H NMR spectrum of benzimidazole **L′** differs significantly from the spectrum of dithioamide **L** (Fig. 6). There is a multiplet at δ 7.34–7.27 which is assigned to the phenyl protons. The N—H resonance for **L** at δ 9.38 is no longer present at **L′**. The *ortho*-aryl protons of **L** assigned as d and e (*δ* 7.62 and 7.53), both split into d and g (*δ* 7.95 and 7.39) and e, f (*δ* 7.53 and 7.42), for **L′** (Fig. 6). Fig. 7 depicts the ^{1}H NMR spectrum of **L** after addition of $HgCl_2$ (1.2 eq.), in comparison with the spectra of **L** (3.2 mM) and **L** with DIPEA (7.0 mM) (bottom, top and middle respectively). After Hg(II) addition the formation of a new species is clearly indicated, with chemical shifts at 8.06, 7.45, and 7.28 ppm, which are substantially different than the benzimidazole **L′**. Resonances for the deprotonated ligand are still prominent, however, indicating that the formation of the transient Hg(II) complex (Scheme 2) is a slow step in the process.

3.5. Single crystal X-ray crystallography

Crystal data, data collection and structure refinement details are summarized in Table 1. The dithioamide compound **L** was solved and refined in a Triclinic, *P-1* space group, with a full molecule in the asymmetric unit (as shown in Fig. 8). The phenyl group of the *o*-phenylenediamine motif (constituted by C1, C2, C3, C4, C5, C6 atoms) is satisfactorily planar with mean deviation of 0.11 (3) Å. The two other dangling phenyl groups constituted by C8, C9, C10, C11, C12, C13 and C15, C16, C17, C18, C19, C20 atoms show excellent planarity (mean deviation, 0.003 (2) Å). The dihedral angles between the two planes constituted by these two phenyl rings with the phenyl ring of the *o*-phenylenediamime motif are 55.8 and 82.8° respectively. The asymmetric unit displays an intramolecular H-bonding interaction of N—H…S, type involving an S atom associated with a thioamide and an amide N—H, that is a part of another thioamide. Examination of the packing pattern for **L** (Fig. 9) revealed that its extended structure is consolidated by several classical H-bonding interactions (N1—H1—S2, with H—S, 2.39 Å; N2—H2—S1, with H—S, 2.67 Åi; C5—H5—S1, with H—S, 2.87 Å; C9—H9—S1, with H—S, 2.65 Å; C16—H16—S2, with H—S, 2.74 Å; Symmetry code: (i) $-x + 1, -y + 2, -z + 1$). The cyclized

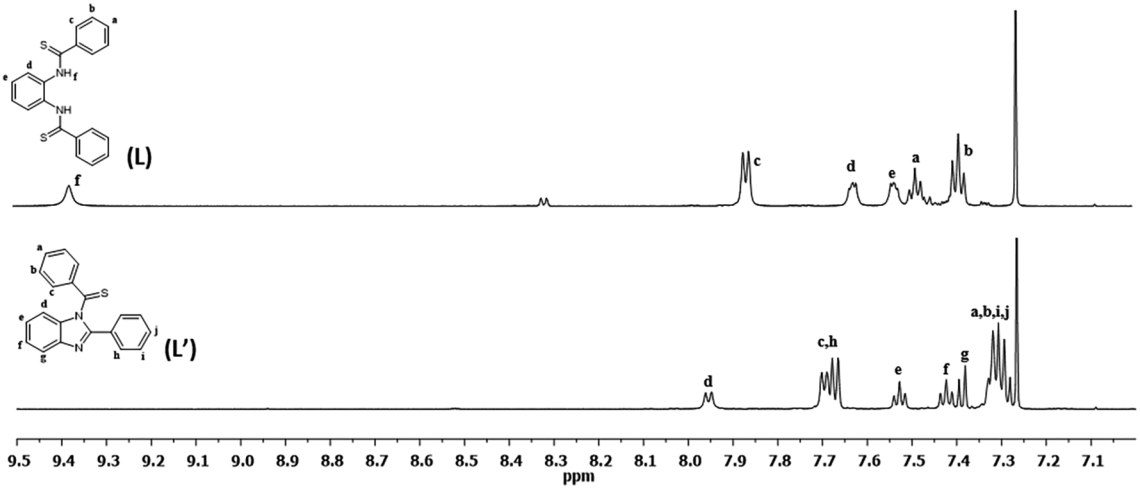

Fig. 6. ^{1}H NMR spectra of di-thioamide (**L**) and the cyclized benzimidazole product (**L′**) in $CDCl_3$.

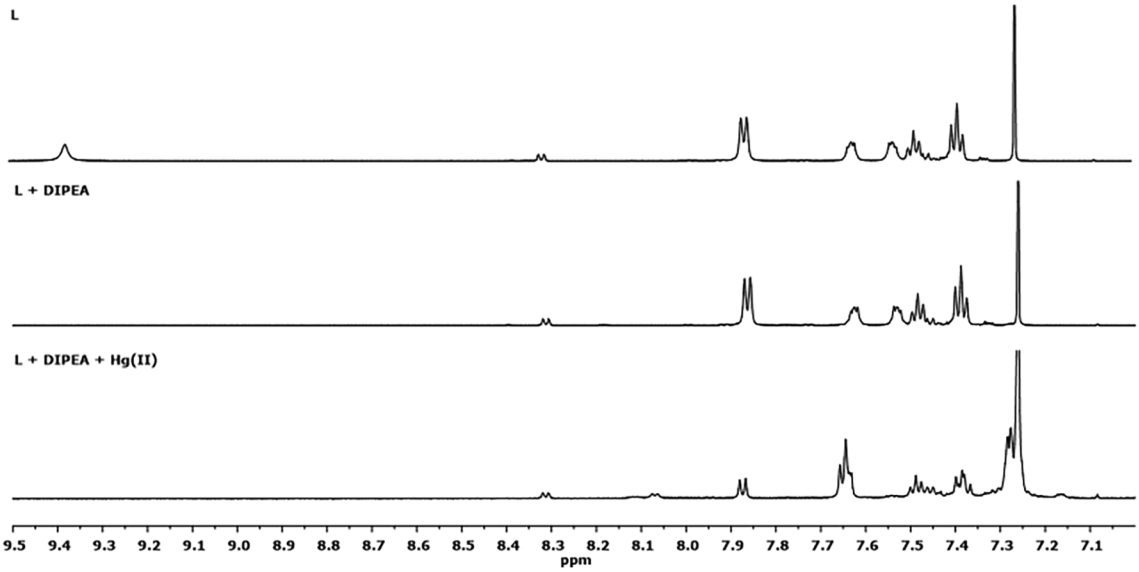

Fig. 7. ^{1}H NMR spectra of **L** (3.2 mM) (top) in comparison with **L** + DIPEA (2.2 eq.) (middle) and the reaction mixture after addition of $HgCl_2$ (1.2 eq.) showing the transient Hg(II)-**L** complex formation at 8.06, 7.45, and 7.28 ppm (bottom).

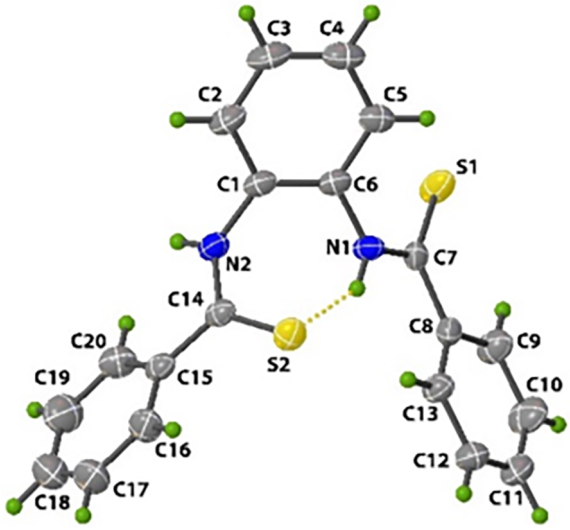

Fig. 8. ORTEP representation (50% probability ellipsoids) for the X-ray crystal structure of dithioamide **L**, with atom labeling scheme, showing an N—H…S intramolecular hydrogen bonding interaction.

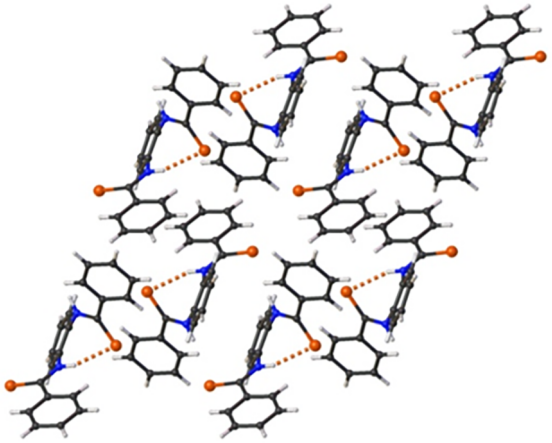

Fig. 9. Packing pattern of L along *a* axis. The dotted lines indicate both intra- and inter-molecular H-bonding interactions.

benzimidazole **L′** (Fig. 10) was obtained from compound **L** through a mercury (II) mediated cyclization process (*vide infra*). The benzimidazole fragment (constituted by C1, C2, C3, C4, C5, C6, C7, N2, N1 atoms) in this compound is satisfactorily planar with mean deviation of 0.017 (3) Å. The conjoining phenyl ring (constituted by C8, C9, C10, C11, C12, C13 atoms) shows excellent planarity (mean deviation, 0.005 (3) Å) and the dihedral angle between this plane and the benzimidazole fragment is 43.0°. The other phenyl ring (constituted by C15, C16, C17, C18, C19, C20 atoms) is also highly planar (mean deviation, 0.004 (3) Å) and the dihedral angle between this plane and the plane of benzimidazole ring is 72.7°. In case of **L′**, its extended structure (Fig. 11) is consolidated by few non-classical H-bonding interactions (C16—H16—N1, with H—N, 2.54 Å; C19—H19—N2, with H—N, 2.61 Åi; C20—H20—S1, with H—S, 2.76 Å; Symmetry code: (i) $x, y, z - 1$).

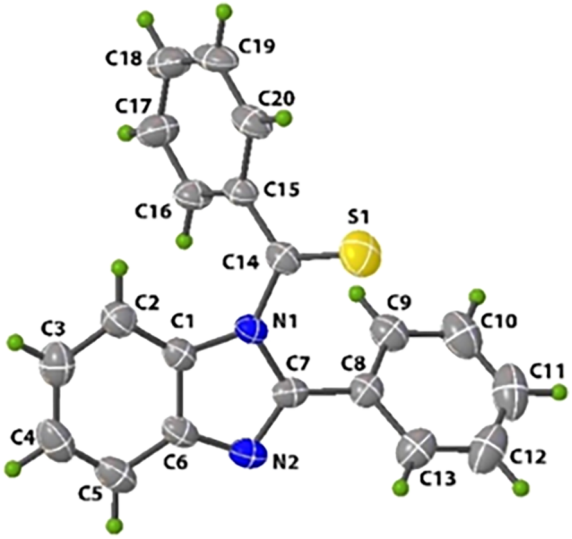

Fig. 10. ORTEP representation (50% probability ellipsoids) for the X-ray crystal structure of benzimidazole **L′**, with atom labeling scheme.

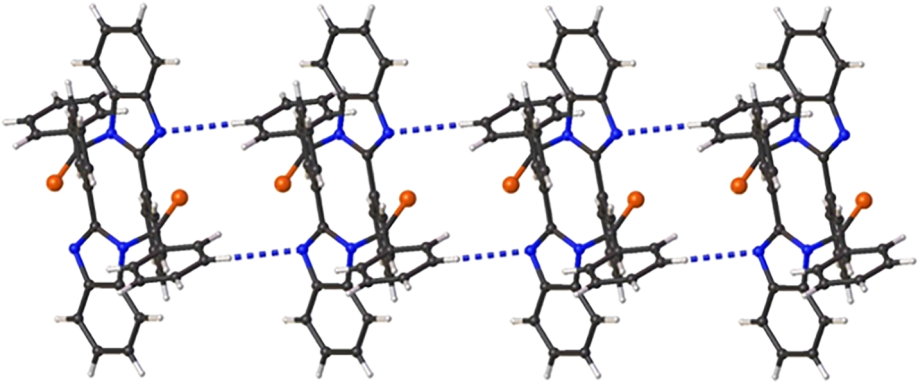

Fig. 11. Packing pattern of **L′** along *b* axis. The dotted lines indicate intermolecular H-bonding interactions.

4. Conclusion

In conclusion we have reported selective Hg(II) sensing via Hg(II)-mediated cyclization of a dithioamide, leading to a new benzimidazole derivative. Both the dithioamide and benzimidazole compounds were fully characterized by X-ray crystallography. The Hg(II)-mediated cyclization is presumed to occur via the formation of a transient Hg(II) thioamide species, which was characterized tentatively by ^{1}H NMR. We expect to continue this study in the future with detailed selectivity studies under competitive conditions in the presence of more complicated metal mixtures and also perform similar studies with substituted derivatives, such as N,N′-(4,5-dimethyl-1,2-phenylene)dibenzothioamide.

Declaration of Competing Interest

The authors declare that they have no known competing financial interests or personal relationships that could have appeared to influence the work reported in this paper.

Acknowledgements

We would like to thank Mr. Omar Fernandez, Mr. Yatfung Chiu, Ms. Maria Fabiola Alvarado-Yepes, and Ms. Naivys Rodriguez for synthetic assistance, and an anonymous reviewer for constructive comments and suggestions. This research project was supported by the US Department of Energy Minority Serving Institution Partnership Program (MSIPP) managed by the Savannah River National Laboratory under SRNS contract BOA No: 541, TOA No. 0000332972 and 0000403067 to FIU. MTF was supported with a scholarship from Nuclear Energy University Programs, Office of Nuclear Energy, US Dept. of Energy, under the DE-NE 0008365 cooperative agreement with FIU.

Appendix A. Supplementary data

Supplementary data including X-ray crystal data for N,N'-(1,2-phenylene)dibenzothioamide (**L**): CCDC 1848353, and Phenyl(2-phenyl-1H-benzimidazol-1-yl)methanethione (**L′**): CCDC 1848354 and additional experimental details to this article can be found online at https://doi.org/10.1016/j.ica.2020.119680.

References

[1] R.A. Bernhoft, Mercury toxicity and treatment: a review of the literature, J. Environ. Public Health 2012 (2012) 460508, , https://doi.org/10.1155/2012/460508.

[2] R. Puk, J.H. Weber, Critical review of analytical methods for determination of inorganic mercury and methylmercury compounds, Appl. Organomet. Chem. 8 (1994) 293–302, https://doi.org/10.1002/aoc.590080404.

[3] K. Tian, G. Siegel, A. Tiwari, A simple and selective colorimetric mercury (II) sensing system based on chitosan stabilized gold nanoparticles and 2,6-pyridinedicarboxylic acid, Mater. Sci. Eng. C 71 (2017) 195–199, https://doi.org/10.1016/j.msec.2016.10.006.

[4] L.N. Suvarapu, S.-O. Baek, Recent developments in the speciation and determination of mercury using various analytical techniques, J. Anal. Methods Chem. 2015 (2015) 372459, , https://doi.org/10.1155/2015/372459.

[5] G.-H. Chen, W.-Y. Chen, Y.-C. Yen, C.-W. Wang, H.-T. Chang, C.-F. Chen, Detection of Mercury(II) ions using colorimetric gold nanoparticles on paper-based analytical devices, Anal. Chem. 86 (2014) 6843–6849, https://doi.org/10.1021/ac5008688.

[6] A.K. Atta, S.-B. Kim, J. Heo, D.-G. Cho, Hg(II)-mediated intramolecular cyclization reaction in aqueous media and its application as Hg(II) selective indicator, Org. Lett. 15 (2013) 1072–1075, https://doi.org/10.1021/ol4000873.

[7] Y. Che, D. Wu, C. Deng, L. Liu, D. Jia, 5-Bromoindole-3-carboxaldehyde ethylthiosemicarbazone for Hg(II) sensing and removal, Chem. Phys. Lett. 644 (2016) 171–175, https://doi.org/10.1016/j.cplett.2015.11.021.

[8] K. Song, J. Mo, C. Lu, Hg(II) sensing platforms with improved photostability: the combination of rhodamine derived chemosensors and up-conversion nanocrystals, Spectrochim. Acta. A. Mol. Biomol. Spectrosc. 179 (2017) 125–131, https://doi.org/10.1016/j.saa.2017.02.034.

[9] K. Kavallieratos, J.M. Rosenberg, W.-Z. Chen, T. Ren, Fluorescent sensing and selective Pb(II) extraction by a dansylamide ion-exchanger, J. Am. Chem. Soc. 127 (2005) 6514–6515, https://doi.org/10.1021/ja050296e.

[10] R.J. Alvarado, J.M. Rosenberg, A. Andreu, J.C. Bryan, W.-Z. Chen, T. Ren, K. Kavallieratos, Structural insights into the coordination and extraction of Pb(II) by disulfonamide ligands derived from o-phenylenediamine, Inorg. Chem. 44 (2005) 7951–7959, https://doi.org/10.1021/ic051103r.

[11] K. Kavallieratos, J.M. Rosenberg, J.C. Bryan, Pb(II) coordination and synergistic ion-exchange extraction by combinations of sulfonamide chelates and 2,2‘-bipyridine, Inorg. Chem. 44 (2005) 2573–2575, https://doi.org/10.1021/ic050047r.

[12] I. Lehman-Andino, J. Su, K.E. Papathanasiou, T.M. Eaton, J. Jian, D. Dan, T.E. Albrecht-Schmitt, C.J. Dares, E.R. Batista, P. Yang, J.K. Gibson, K. Kavallieratos, Soft-donor dipicolinamide derivatives for selective actinide(III)/lanthanide(III) separation: the role of S- vs. O-donor sites, Chem. Commun. 55 (2019) 2441–2444, https://doi.org/10.1039/C8CC07683A.

[13] H.A. Barker, R.D. Smyth, H. Weissbach, J.I. Toohey, J.N. Ladd, B.E. Volcani, Isolation and properties of crystalline cobamide coenzymes containing benzimidazole or 5, 6-dimethylbenzimidazole, J. Biol. Chem. 235 (1960) 480–488.

[14] A.A. Spasov, I.N. Yozhitsa, L.I. Bugaeva, V.A. Anisimova, Benzimidazole derivatives: spectrum of pharmacological activity and toxicological properties (a review), Pharm. Chem. J. 33 (1999) 232–243, https://doi.org/10.1007/BF02510042.

[15] F. Arjmand, B. Mohani, S. Ahmad, Synthesis, antibacterial, antifungal activity and interaction of CT-DNA with a new benzimidazole derived Cu(II) complex, Eur. J. Med. Chem. 40 (2005) 1103–1110, https://doi.org/10.1016/j.ejmech.2005.05.005.

[16] M. Tariq Khan, M. Tahir Razi, S. Jan, M. Mukhtiar, R. Gul, A. Hussain, A. Mehmood Hashmi, M. Taufiq Ahmad, N. Ahmed Shahwani, I. Rabbani, Synthesis characterization and antihypertensive activity of 2-phenyl substituted benzimidazoles, Pak. J. Pharm. Sci. 31 (2018) 1067–1074.

[17] M. Tonelli, M. Simone, B. Tasso, F. Novelli, V. Boido, F. Sparatore, G. Paglietti, S. Pricl, G. Giliberti, S. Blois, C. Ibba, G. Sanna, R. Loddo, P. La Colla, Antiviral activity of benzimidazole derivatives. II. Antiviral activity of 2-phenylbenzimidazole derivatives, Bioorg. Med. Chem. 18 (2010) 2937–2953, https://doi.org/10.1016/j.bmc.2010.02.037.

[18] M. Tonelli, F. Novelli, B. Tasso, I. Vazzana, A. Sparatore, V. Boido, F. Sparatore, P. La Colla, G. Sanna, G. Giliberti, B. Busonera, P. Farci, C. Ibba, R. Loddo, Antiviral activity of benzimidazole derivatives. III. Novel anti-CVB-5, anti-RSV and anti-Sb-1 agents, Bioorg. Med. Chem. 22 (2014) 4893–4909, https://doi.org/10.1016/j.bmc.2014.06.043.

[19] V. Yerragunta, P. Patil, S. Srujana, R. Devi, R. Gayathri, Srujana, A. Divya, Benzimidazole derivatives and its biological importance: a review, PharmaTutor Mag. 2 (2014) 109–113.

[20] J. Peng, M. Ye, C. Zong, F. Hu, L. Feng, X. Wang, Y. Wang, C. Chen, Copper-catalyzed intramolecular C−N bond formation: a straightforward synthesis of benzimidazole derivatives in water, J. Org. Chem. 76 (2011) 716–719, https://doi.org/10.1021/jo1021426.

[21] S.R. Fletcher, E. McIver, S. Lewis, F. Burkamp, C. Leech, G. Mason, S. Boyce, D. Morrison, G. Richards, K. Sutton, A.B. Jones, The search for novel TRPV1-antagonists: from carboxamides to benzimidazoles and indazolones, Bioorg. Med. Chem. Lett. 16 (2006) 2872–2876, https://doi.org/10.1016/j.bmcl.2006.03.004.
[22] D. Ma, Q. Cai, Copper/amino acid catalyzed cross-couplings of aryl and vinyl halides with nucleophiles, Acc. Chem. Res. 41 (2008) 1450–1460, https://doi.org/10.1021/ar8000298.
[23] M. Adharvana Chari, D. Shobha, T. Sasaki, Room temperature synthesis of benzimidazole derivatives using reusable cobalt hydroxide (II) and cobalt oxide (II) as efficient solid catalysts, Tetrahedron Lett. 52 (2011) 5575–5580, https://doi.org/10.1016/j.tetlet.2011.08.047.
[24] H. Alinezhad, F. Salehian, P. Biparva, Synthesis of benzimidazole derivatives using heterogeneous ZnO nanoparticles, Synth. Commun. 42 (2012) 102–108, https://doi.org/10.1080/00397911.2010.522294.
[25] G. Biswas, S. Ghorai, A. Bhattacharjya, Mercuric chloride and iodide mediated cyclization of tethered alkynedithioacetals as a general route to five- and six-membered rings: tuning of regioselectivity by alkyne substitution, Org. Lett. 8 (2006) 313–316, https://doi.org/10.1021/ol0527274.
[26] S. Ghorai, A. Bhattacharjya, Mercury(II) chloride-mediated cyclization – rearrangement of O-propargylglycolaldehyde dithioacetals to 3-pyranone dithioketals: an Expeditious access to 3-pyranones, Org. Lett. 7 (2005) 207–210, https://doi.org/10.1021/ol047893a.
[27] Y.-S. Su, M.-J. Lin, M.-C. Sun, Mercury chloride assisted cyclization toward benzimidazoles by focused microwave irradiation, Tetrahedron Lett. 46 (2005) 177–180, https://doi.org/10.1016/j.tetlet.2004.10.170.
[28] J. Wang, Z. He, X. Chen, W. Song, P. Lu, Y. Wang, Efficient access to polysubstituted amidines, benzimidazoles and pyrimidines from amides, Tetrahedron 66 (2010) 1208–1214, https://doi.org/10.1016/j.tet.2009.12.034.
[29] I. Azumaya, I. Okamoto, S. Nakayama, A. Tanatani, K. Yamaguchi, K. Shudo, H. Kagechika, A chiral N-methylbenzamide: spontaneous generation of optical activity, Tetrahedron 55 (1999) 11237–11246, https://doi.org/10.1016/S0040-4020(99)00647-X.
[30] Y. Zhu, L. Chuanzhao, A.O. Biying, M. Sudarmadji, A. Chen, D.T. Tuan, A.M. Seayad, Stabilized well-dispersed Pd(0) nanoparticles for aminocarbonylation of aryl halides, Dalton Trans. 40 (2011) 9320–9325, https://doi.org/10.1039/c1dt10927h.
[31] F.M. Moghaddam, H.Z. Boeini, Oxidative cyclization of thiobenzanilides to benzothiazoles using N-Benzyl-DABCO tribromide under mild conditions, Synlett 2005 (2005) 1612–1614, https://doi.org/10.1055/s-2005-869841.
[32] B.S. Pedersen, S. Scheibye, N.H. Nilsson, S.-O. Lawesson, Studies on organophosphorus compounds XX. syntheses of thioketones, Bull. Sociétés Chim. Belg. 87 (1978) 223–228, https://doi.org/10.1002/bscb.19780870310.
[33] G.M. Sheldrick, Crystal structure refinement with SHELXL, Acta Crystallogr. Sect. C Struct. Chem. 71 (2015) 3–8, https://doi.org/10.1107/S2053229614024218.
[34] O.V. Dolomanov, L.J. Bourhis, R.J. Gildea, J.a.K. Howard, H. Puschmann, OLEX2: a complete structure solution, refinement and analysis program, J. Appl. Crystallogr. 42 (2009) 339–341, https://doi.org/10.1107/S0021889808042726.